Analytical Longitudinal Speed Planning for CAVs with Previewed Road Geometry and Friction Constraints

Liming Gao, Craig Beal, *IEEE Member,* Daniel Fescenmyer, Sean Brennan*, IEEE Member*

***Abstract*— Due to the lack of information, current vehicle control systems generally assume that the road friction conditions ahead of a vehicle are unchanged relative to those at the vehicle's current position. This can result in dangerous situations if the friction is suddenly decreasing from the current situation, or overly conservative driving styles if the friction of the current situation is worse than the roadway ahead. However, with connectivity either to other vehicles, infrastructure, or cloud services, future vehicles may have access to upcoming roadway information; this is particularly valuable for planning velocity trajectories that consider the friction and geometry in the road path ahead. This paper introduces a method for planning longitudinal speed profiles for Connected and Autonomous Vehicles (CAVs) that have previewed information about path geometry and friction conditions. The novelty of this approach is to explicitly include consideration of the friction ellipse available along the intended path. The paper derives an analytical solution for certain preview cases that upper-bounds the allowable vehicle velocity profile while preventing departure from the friction ellipse. The results further define the relationship between a lower bound on friction, the path geometry, and minimum friction preview distance. This relationship is used to ensure the vehicle has sufficient time to take action for upcoming hazardous situations. The efficacy of the algorithm is demonstrated through an application case where a vehicle navigates a curving road with changing friction conditions, with results showing that, with sufficient preview, the vehicle could anticipate allowable and stable path keeping speed.**

I. Introduction

Unforeseen hazardous road conditions such as snow, ice, rain, etc. can have a significant negative impact on vehicle safety and mobility. The Federal Highway Administration reports that approximately 20% of all crashes occur in adverse road conditions; light rain or snow can reduce average traffic flow volume by 5% to 10% on the highway [1]. But assuming worst-case conditions and driving very slowly is not an ideal solution; to maximize the throughput of the highway, vehicles should travel as expediently as possible. Further, even if road conditions are known, another question arises: how far ahead of a vehicle must data be known in order to make appropriate speed-keeping decisions now, in anticipation of the conditions of the road ahead?

Much research has been conducted to address the vehicle mobility issue in hazardous conditions. For example, Advanced Driver Assistance Systems (ADASs) such as EBS, LKA, and ESC, etc. can assist a driver to follow the desired path stably in hazardous situations [2]. These assistance control systems generally operate using information only from the vehicle's measurements and can be categorized into lateral control, longitudinal control, and hybrid control. For example, after a vehicle encounters poor friction conditions and experiences instability, a controller can output a proper steering angle and/or driving/braking torque command to stabilize the motion. An example of this is the work by Yu, et al. which designed a feedback-feedforward steering controller to improve the vehicle stability when employing hard-braking maneuvers on road with split friction [3]. Similarly, Li, et al. presented a torque control strategy for the situation of abrupt changing of road friction [4]. However, most of these controllers are activated after vehicle states have a significant deviation from the nominal value, e.g. in feedback response to situations encountered. With significant and rapid changes in operating conditions such as a curve ahead with reduced friction, the vehicle may be at such a speed that even these advanced control systems are insufficient.

In contrast with these control strategies that react to certain measured vehicle instabilities, researchers have also developed preview-based envelope controllers which can be combined with real-time road friction estimation to keep the vehicle within a stable region bounded by road-tire friction limits. Similar to the feedback methods mentioned earlier, these systems seek to maintain vehicle stability from the perspective of body-fixed state [5]–[7]. However, abrupt changes in road conditions can still require significant preview to anticipate necessary velocity reductions and the necessary preview can be unclear.

Another method of proactively maintaining vehicle stability is to utilize longitudinal velocity planning, e.g. to slow down prior to dangerous situations. This allows a vehicle to maintain stability when following a path with tight curvature change [2]. This mitigates the need for the vehicle to react as aggressively during the onset of instability because, when operating with lower velocities, vehicles generally have a larger stable operating region and can reserve tire forces to follow the desired path [4][5].

However, previously published longitudinal velocity planning approaches typically consider only the variation of

Liming Gao is a graduate student in Department of Mechanical Engineering at The Pennsylvania State University, University Park, PA 16802, USA (e-mail: lug358@ psu.edu).

Craig Beal is with Department of Mechanical Engineering, Bucknell University, Lewisburg, PA 17837, USA (e-mail: cbeal@bucknell.edu). IEEE Member.

Daniel Fescenmyer is an undergraduate student in Department of Mechanical Engineering at The Pennsylvania State University, University Park, PA 16802, USA (e-mail: dzf5248@psu.edu).

Sean Brennan is with the Department of Mechanical Engineering, The Pennsylvania State University, University Park, PA 16802, USA (e-mail: sbrennan@psu.edu). IEEE Member.

Manuscript 926 submitted to 2021 IEEE International Intelligent Transportation Systems Conference (ITSC). Received April 20, 2021.

path curvature, and little attention has been paid to the road surface friction condition changing when conducting longitudinal velocity planning. Research has proved that prior estimation of friction and peak tire force before a slick region is reached allows a vehicle chassis control system to work more reliably and proactively [2]. As a result, if the vehicle can preview the path friction reduction and slow down appropriately before entering the slick region, even a simple proportional lookahead steering controller [10] can operate the vehicle to follow the desired path well.

One potential solution to preview the road surface friction condition is motivated by the increasing development of Connected and Autonomous Vehicles (CAVs) which can utilize both network intelligence and individual intelligence, where road friction information [11] from the individual vehicles and/or roadside sensor units is shared between vehicle to vehicle, vehicle to infrastructure, and/or vehicle to database systems. In this way, each vehicle in the network could query the aggregated friction information from the shared database. An illustration of this network framework is shown in Fig. 1.

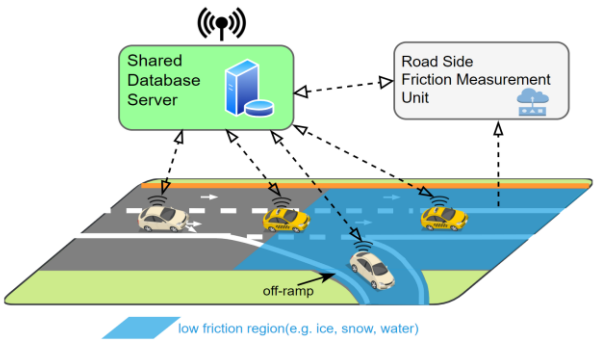

Figure 1. A strategy of road friction and geometry preview with a shared roadway database. The shared database can leverage network intelligence to substantially improve the operation of each individual in the population.

In this paper, an idea of road friction preview through database-informed CAVs is introduced, inspired by the work of various authors on vehicle dynamics at the limits of handing [6], [12], [13]. Specifically, this work presents an algorithm to generate a longitudinal vehicle velocity limit profile for a given desired path that takes into account local speed limits, road geometry, and current road friction conditions. Closed-form analytical formulae are established for certain preview cases, allowing for the introduction of a straightforward and efficient algorithm for generating the velocity profile. Furthermore, relationships are established between a lower bound on the friction along the path, the path geometry, and minimum friction preview distance that ensure a human driver or autonomous vehicle has sufficient time to take action for upcoming hazardous situations.

The remainder of this paper is organized as follows: Section II discusses the velocity limit profile planning based on the road-tire friction limits and road geometry. Section III analyzes the friction preview distance. Section IV demonstrates the approach with an application case. Finally, Section V summarizes the main results of the work.

II. Vehicle Longitudinal Velocity Planning Given a Reference Path

This section presents the generation of a limit speed profile that vehicles can achieve without exceeding available tire friction limits constraints. The section begins by deriving the constraints of driving on the friction circle by controlling the vehicle longitudinal dynamics, and then introduces an approach to describe a driving path by station s, curvature κ, and friction coefficient μ. Finally, the section concludes with the details of the velocity planning method.

A. Vehicle Chassis Model and Tire Friction Limits

The vehicle dynamic equations for the three-state single track model shown in Fig. 2 are:

$$\dot{U}_x = \frac{F_{xf}\cos(\delta) - F_{yf}\sin(\delta) + F_{xr}}{m} + rU_y - g\sin(\theta) \quad (1)$$

$$\dot{U}_y = \frac{F_{yf}\cos(\delta) + F_{xf}\sin(\delta) + F_{yr}}{m} - rU_x \quad (2)$$

$$\dot{r} = \frac{a(F_{yf}\cos(\delta) + F_{xf}\sin(\delta)) - bF_{yr}}{I_{zz}} \quad (3)$$

where longitudinal velocity U_x, lateral velocity U_y, and yaw rate r are the three states. θ is the path grade, and g is the gravitational acceleration. The vehicle parameters include the vehicle mass m, yaw moment of inertia I_{zz}, front wheel steering angle δ, and a and b the distances from the vehicle's center of gravity to the front and rear axle respectively. F_{xf}, F_{xr}, F_{yf}, F_{yr} are the longitudinal and lateral forces acting on the front and rear tires.

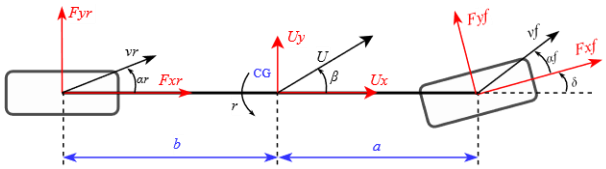

Figure 2. Planar single-track vehicle chassis model

The maximum available longitudinal force F_x and lateral force F_y at each tire is constrained by a circular friction constraint:

$$F_{xi}^2 + F_{yi}^2 \le \left(\mu F_{zi}\right)^2; \quad i = f,r. \quad (4)$$

where μ is the road-tire friction coefficient, and F_{zf} and F_{zr} are the vertical force at the front and rear axle respectively. Ignoring the effects of lateral and longitudinal load transfer, the vertical forces can be expressed as $F_{zf} = mg\cos(\theta)b/(a+b)$ and $F_{zf} = mg\cos(\theta)a/(a+b)$

Determining the limit speed profile requires the vehicle to utilize all the available tire friction to generate forces so that vehicle can operate at the acceleration limits to achieve the maximum safe speed [14], [15]. It implies that all tire forces need to remain on the boundary of the friction circle, i.e. equality holds in (4).

Manuscript 926 submitted to 2021 IEEE International Intelligent Transportation Systems Conference (ITSC). Received April 20, 2021.

Fig. 3 shows the road-tire force when maneuvering through a left corner of a path at the tire limits. The boundary of the friction circle depends on the road-tire friction coefficient.

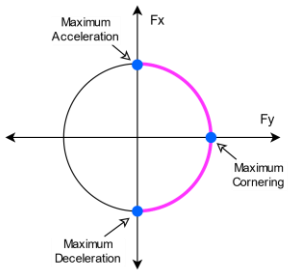

Figure 3. The maximum performance of vehicle can be achieved by driving at the boundary of friction circle. This plot shows the left cornering case.

As this work is interested in the longitudinal dynamics of a vehicle traveling stably along a path, the lateral and rotational state derivatives are assumed to be zero with the quasi-steady value of the rotational velocity dictated by the road geometry. The lateral velocity is assumed to be approximately zero, yielding:

$$\dot{V}_y = 0, \quad \dot{r}=0, \quad U_y=0, \quad r=\kappa U_x \tag{5}$$

where κ is the path curvature.

Substituting (4) with equality condition and (5) into (1), (2), and (3) yields:

$$\dot{U}_x = \pm\sqrt{\left(\mu g\cos(\theta)\right)^2 - \left(\kappa U_x^2\right)^2} \pm g\sin(\theta), \tag{6}$$

a basic version of the key equation governing the longitudinal speed while operating at the friction limits on a path of known curvature. However, an adjusting parameter λ is added into the equation (6) to allow for compensation of the uncertainty of friction preview, the assumptions of the derivation, and the fact that most drivers may not be comfortable with or able to operate a vehicle at the friction limits as racing drivers or autonomous driving systems might [5]. Consequently, the dynamic equation that depicts the maximum available longitudinal acceleration is expressed as:

$$\dot{U}_x = \pm\sqrt{\left(\lambda\mu g\cos(\theta)\right)^2 - \left(\kappa U_x^2\right)^2} \pm g\sin(\theta) \tag{7}$$

where the plus-minus sign (±) corresponds to acceleration and deceleration respectively. Positive θ corresponds to upgrades and negative is for downgrades. The parameters μ and κ in (6) depend on the path station position, which is introduced in the following section.

B. Path Representation

In contrast to many publications that describe the process of path planning for minimal time or maximal speed within the boundaries of a road or track, this paper instead focuses on following a given path. Specifically, the emphasized use is for following the lane centerline of a given highway with occasional vehicle-planned lane changes. Therefore, the desired path is assumed to be known. A clothoid path description is widely used for highway road design [16] and vehicle path planning, for example, the racing line [17], [18] and minimum curvature optimal path [19],[20]. A clothoid path can generally be described by a succession of turns – consisting of spirals and constant radius arcs – and straight lines. The spiral segments are defined to have linearly increasing or decreasing curvature along the path:

$$\kappa = (\kappa_c / L_s)s \tag{8}$$

where s referred to as "station" in this paper, is the distance measured along a path; L_s is the total length of the spiral and κ_c is the curvature at the end of the spiral. In this way, the curvature of the whole path can be described by a sequence of linear functions.

Without loss of generality, an example oval path similar to the Larson Institute Test Track [21] is shown in Fig. 4. The path is given according to the highway road design rule which decomposes the corner into three phases: an entry clothoid, a circular arc, and an exit clothoid [18]. The corresponding curvature, along with the road grade and a hypothetical friction profile, are shown in Fig. 5. All of these path parameters can be described as a function of the path station: $\kappa(s)$, $\mu(s)$, $\theta(s)$. The path segments where the grade is non-zero were chosen to be similar to the off-ramp and on-ramp parts of a highway.

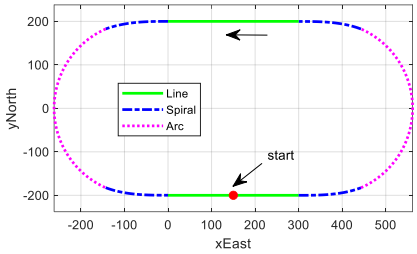

Figure 4. A circular oval smaple path.

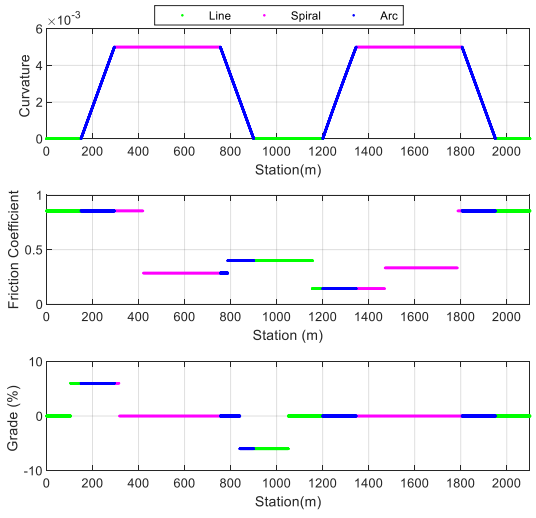

Figure 5. The curvature, previewed friction coefficient, and previewed grade for the sample path. The friction is assumed to change abruptly.

C. Velocity Profile Generation

Velocity planning has a significant impact on driving safety, especially when vehicles drive on a road with changing friction and geometry. With the longitudinal dynamic equation

(7) and the desired path description, the speed profile can be determined. The approach presented in this paper is inspired by previous work that addressed the profile determination via three passes [15], nonlinear optimization [2], and segment and iteration [22], where a velocity profile is planned given the path curvature.

Express the longitudinal acceleration with respect to the path station:

$$\dot{U}_x = \frac{dU_x}{dt} = \frac{dU_x}{ds}\frac{ds}{dt} = \frac{dU_x}{ds}U_x \tag{9}$$

Substituting (9) into (7) yields:

$$\frac{dU_x(s)}{ds} = \frac{1}{U_x(s)}\left(\pm\sqrt{\left(\lambda\mu(s)g\cos(\theta)\right)^2 - \left(\kappa(s)U_x^2(s)\right)^2} \pm g\sin(\theta)\right) \tag{10}$$

A closed-form solution for (10) can be solved for straight line and circular arc segments, which generally account for the majority of real-world roadway designs. For the straight line segment with constant friction, the solution of (10) is:

$$U_{x\_l}^2 = 2\left(\pm\lambda\mu g\cos(\theta) \pm g\sin(\theta)\right)s + U_{x\_l0}^2 \tag{11}$$

where U_{x_l0} is the initial speed condition. As well, for the zero-grade radius arc path whose curvature and friction coefficient are constant, (10) can again be solved analytically:

$$\mathrm{U}_{x\_a}(\mathrm{s}) = \frac{\sqrt{\lambda\mu g/\kappa}\sqrt{\pm\tan\left(2(s\pm c1)\kappa\right)}}{\sqrt[4]{\tan^2\left(2(s-c1)\kappa\right)+1}} \tag{12}$$

where $c1 = \frac{1}{2\kappa}\tan^{-1}\frac{U_{x\_a0}^2}{\sqrt{\left(\lambda\mu g/\kappa\right)^2 - U_{x\_a0}^4}}$ is a parameter depending on the initial speed condition U_{x_a0}.

For spiral and arc path with a non-zero grade, (10) is hereafter solved via ODE solvers in this work, using a numerical Runge-Kutta (4,5) method as it is more accurate than Euler's method often used for similar problems [15].

Based on the solution analysis above, the first step of generating the speed profile is to divide the given path into piecewise segments with linear or constant curvature and constant friction and grade.

The second step is to, along each segment, find the maximum permissible steady-state vehicle velocity with zero longitudinal acceleration, which is given by (13):

$$U_x(s) = \sqrt{\lambda\mu(s)g/\kappa(s)}\,. \tag{13}$$

Notice that the steady-state speed will be very high when the curvature is small; if the curvature is zero, this yields an infinite maximum curve speed for a straight line, and thus a speed limit of 50m/s is imposed (actual road speed limits could also be used for highways) for this work. A factor λ=0.95 is also chosen to explore the vehicle behavior close to the friction limits. The result of this step is the "curve limit speed" as shown in Fig. 6(a).

The next step is a forward speed limit calculation step which constrains accelerations. This calculation starts from the first segment with the initial speed at s = 0. Then for each following segment, the speed planning proceeds using (11), (12) or a numerical method, where the initial speed is determined by the exit speed of the previous segment. A key point of this step is that the speed result at each segment is compared to the curve limit speed, and the minimum value is taken. This step indicates how fast a vehicle can accelerate with path constraints, as shown as the "forward limit" in Fig. 6(a).

Next, the backward speed limit calculation occurs. It starts from the last path segment and takes the desired vehicle speed at the end of the path as the initial speed condition. Then the speed profile for each preceding segment is calculated until the vehicle reaches the first path segment. The result at each segment is also compared to the curve limit speed and takes the minimum. This backward calculation indicates the speed limits such that the vehicle can sufficiently decelerate, as shown as the "backward limit" in Fig. 6(a). Finally, the minimum of the "backward limit" and the "forward limit" is used as the final speed profile shown as the "combined results" in Fig. 6(a).

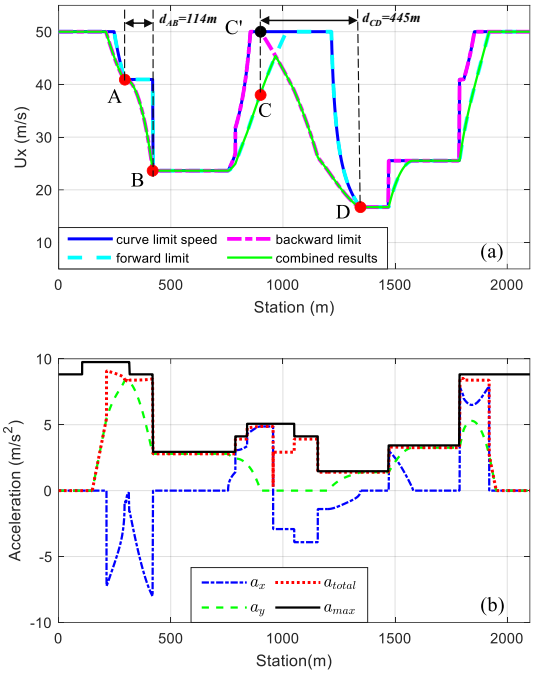

Figure 6. (a) The intermediate and final results of the speed profile of the computation algorithm. (b) The acceleration of the speed profile.

The corresponding acceleration profile is shown in Fig. 6(b) indicating that the total acceleration used by the vehicle:

$$a_{total} = \sqrt{a_x^2 + a_y^2} \tag{14}$$

is bounded by the friction limit and road grade:

$$a_{\max} = \mu g\cos(\theta) + g\left|\sin(\theta)\right|. \tag{15}$$

Additionally, note that in this case the acceleration value is large especially at the high friction region, but the acceleration value can be tailored by choosing a proper adjusting factor λ.

In summary, the feasible speed trajectories and associated preview are determined as follows:

1) Given a path with position s and curvature κ, the corresponding friction μ and grade θ are found far

ahead of the vehicle, much farther than the possible minimum look-ahead distance. These values are assumed to be stored either on the vehicle or obtained in advance via V2x communication. In the example above, 2.1 km is used.

2) Break the path ahead of the vehicle into piecewise segments according to curvature, friction, and grade.

3) The steady-state curve limit speed is found for each segment as calculated by (13).

4) Starting at s=0 and stepping in the forward direction, the possible change in speed is calculated using (11), (12) or a numerical method so that the friction ellipse and road grade constraints are not violated.

5) Next, starting at $s = s_{\text{final}}$ and stepping in the reverse direction, the change in speed is calculated from (11), (12) or a numerical method.

6) The minimum speeds from steps 4 and 5 are used as the final limit speed profile.

III. Minimum Friction Preview Distance

Examining Fig. 6, one can see that the speed profile calculated at each station requires information ahead of the station, but the distance ahead changes at each station depending on conditions. For example, to correctly calculate the velocity limits at station A, the path information at station B (114m ahead of A) must be known. Similarly, the determination of speed limit at C even requires the information at location D (445 m ahead of C). We call this required information window the minimum preview distance.

Examining Fig. 6 again, the preview information is only required at the path region where the "backward limit" speed profile is lower than the curve limit speed profile. It implies that the preview information is necessary to enable the vehicle to make anticipation and decelerate sufficiently before reaching an upcoming hazardous situation. With this observation, the preview region can be extracted from the speed profile, and thereby the minimum preview distance at each station can be calculated easily. Fig.7. presents the results for the path situations shown in Fig.5. It can be observed that the preview distance at station C is noticeably large; this is because station C is a position approaching a high curvature region with low friction.

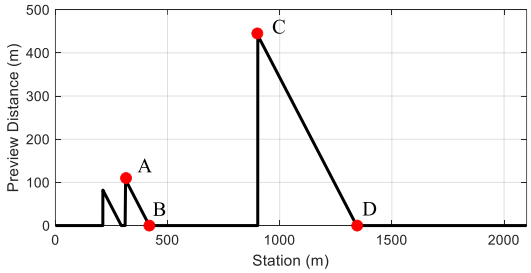

Figure 7. The minimum preview distance for sample-path shown as

When friction information is collected via a system outside the vehicle, for example, a shared database, the use of an appropriate preview distance is important to prevent unnecessary transmission of large amounts of data. Longer preview distances involve more data transmission, resulting in more time delay and data cost, but an overly short preview distance could lead to a situation where a vehicle might not have enough space to respond to the dangerous situation ahead. Therefore, the database or the vehicle should be able to host algorithms that calculate the minimum preview horizon.

In application, the preview distance needs to be determined before querying friction data from a database. One means to proceed is to first assume a constant low friction bound for the initial query. This bound may be provided by the database, given the aggregation of data, but can also be estimated on each vehicle individually. For example, when driving during adverse weather such as rain and snow, a very low road friction bound and thereby a long friction preview distance is expected; but driving during a clear sunny day, the friction bound should be larger and may require very little, perhaps zero, preview. This dependency of preview distance on friction bound is illustrated in Fig. 8. Fig.8 also reveals that the large preview distance occurs at the locations approaching the turns of a path, for example, the path segment before s=1400m, whereas the locations far after the turns would not require any preview, for example, the path segment after s=1500m. The locations requiring large preview distance imply the potentially dangerous parts of a driving path.

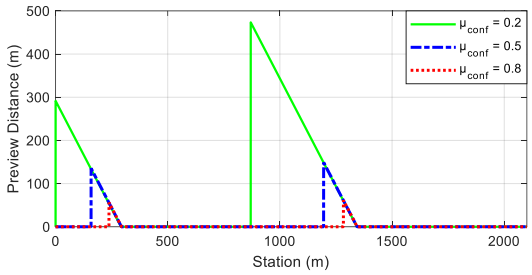

Figure 8. The minimum preview distance versus station and low friction bound for sample-path shown in Fig. 4.

IV. Application Case and Simulation Results

This work presents an application case to demonstrate the efficacy of the preview speed planning algorithm. In this case, a vehicle follows the path shown in Fig. 4 with the hypothetical station-dependent friction conditions given in Fig. 5.

In this simulation case, a driver model is used based on the assumption that a driver intends to look ahead with a 20m horizon when tracking the desired path [10]. A 7-DOF rear-wheel-drive and front steering vehicle model [8] is used for the chassis dynamics. A conservative value of adjustment factor λ=0.4 is chosen to account for the fact that the rear-wheel-drive vehicle does not split the driving force evenly between the two axles and also to model a non-aggressive, cautious driver style.

Fig.9 presents the path tracking performances of lateral error and speed profile. Fig. 9(b) shows that the vehicle with the preview algorithm for allowable curve-keeping speed can anticipate and conduct necessary speed changes, but the other vehicle without speed preview only starts to change speed when a friction decreasing situation is encountered. Consequently, the speed preview algorithm enables the vehicle to adjust speed proactively and track the desired path successfully with acceptable lateral error, but the vehicle

without preview fails to track the path and even departs from the path resulting in a crash, shown in Fig. 9(a). This demonstrates that the speed planning with the preview of road friction and geometry could provide significant benefit for driving performance.

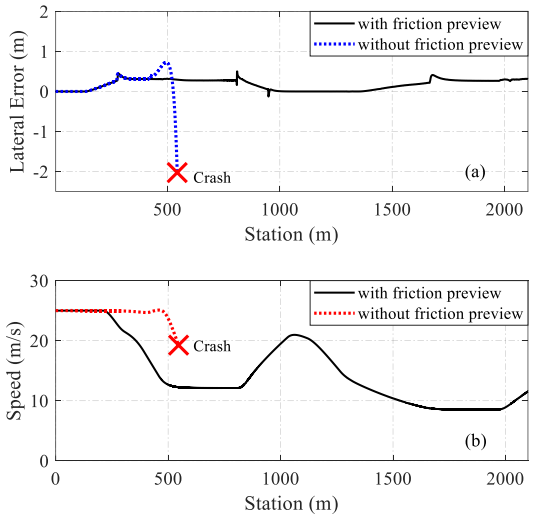

Figure 9. Path tracking performances for the situation with and without friction preview: (a) Lateral tracking error (b) Vehicle speed.

V. Conclusion

This paper presents a method for planning longitudinal speed profiles for CAVs that have previewed information about road geometry and friction conditions. The idea of preview is to extend individual intelligence with network intelligence. The longitudinal speed planning is enabled by solutions to the allowable velocity profile that prevents departure from the friction ellipse with closed-form analytical results in certain cases. The results further define the relationship between the minimum preview distance and longitudinal velocity limits that ensure the vehicle has sufficient time to take action for upcoming hazardous situations. The efficacy of the algorithm is demonstrated through an application case where a vehicle navigates curvy roads with changing friction conditions at allowable and stable speeds.

Acknowledgment

This material is based upon work supported by the National Science Foundation under grant numbers CNS-1932509, CNS-1931927, CNS-1932138 “CPS: Medium: Collaborative Research: Automated Discovery of Data Validity for Safety-Critical Feedback Control in a Population of Connected Vehicles”.

References

[1] A. F. Highway, “How Do Weather Events Impact Roads?,” 2020. https://ops.fhwa.dot.gov/weather/q1_roadimpact.htm (accessed Apr. 08, 2021).

[2] H. Cao, X. Song, S. Zhao, S. Bao, and Z. Huang, “An optimal model-based trajectory following architecture synthesising the lateral adaptive preview strategy and longitudinal velocity planning for highly automated vehicle,” Veh. Syst. Dyn., vol. 55, no. 8, pp. 1143–1188, 2017, doi: 10.1080/00423114.2017.1305114.

[3] L. Yu, S. Zheng, Y. Dai, L. Abi, X. Liu, and S. Cheng, “A feedback-feedforward steering controller designed for vehicle lane keeping in hard-braking manoeuvres on split-μ roads,” Veh. Syst. Dyn., 2021, doi: 10.1080/00423114.2020.1869274.

[4] L. Li, “PID plus fuzzy logic method for torque control in traction control system,” Int. J. Automot. Technol., vol. 13, no. 3, pp. 441–450, 2012, doi: 10.1007/s12239.

[5] C. E. Beal and J. C. Gerdes, “Model predictive control for vehicle stabilization at the limits of handling,” IEEE Trans. Control Syst. Technol., vol. 21, no. 4, pp. 1258–1269, 2013, doi: 10.1109/TCST.2012.2200826.

[6] J. Ni, J. Hu, and C. Xiang, “Envelope Control for Four-Wheel Independently Actuated Autonomous Ground Vehicle Through AFS/DYC Integrated Control,” IEEE Trans. Veh. Technol., vol. 66, no. 11, pp. 9712–9726, 2017, doi: 10.1109/TVT.2017.2723418.

[7] D. Efremov, M. Klauco, T. Hanis, and M. Hromcik, “Driving Envelope Definition and Envelope Protection Using Model Predictive Control,” in 2020 American Control Conference (ACC), 2020, pp. 4875–4880, doi: 10.23919/ACC45564.2020.9147211.

[8] C. E. Beal and C. Boyd, “Coupled lateral-longitudinal vehicle dynamics and control design with three-dimensional state portraits,” Veh. Syst. Dyn., vol. 57, no. 2, pp. 286–313, 2019, doi: 10.1080/00423114.2018.1467019.

[9] C. G. Bobier-Tiu, C. E. Beal, J. C. Kegelman, R. Y. Hindiyeh, and J. C. Gerdes, “Vehicle control synthesis using phase portraits of planar dynamics,” Veh. Syst. Dyn., vol. 57, no. 9, pp. 1318–1337, 2019, doi: 10.1080/00423114.2018.1502456.

[10] K. Hasegawa and E. Konaka, “Three look-ahead distance scheme for lateral control of vision-based vehicles,” Proc. SICE Annu. Conf., pp. 660–665, 2014, doi: 10.1109/SICE.2014.6935214.

[11] C. E. Beal, “Rapid Road Friction Estimation using Independent Left/Right Steering Torque Measurements,” Veh. Syst. Dyn., vol. 58, no. 3, pp. 377–403, 2020, doi: 10.1080/00423114.2019.1580377.

[12] J. Subosits and J. C. Gerdes, “Autonomous vehicle control for emergency maneuvers: The effect of topography,” in 2015 American Control Conference, 2015, pp. 1405–1410, doi: 10.1109/ACC.2015.7170930.

[13] K. Kritayakirana and J. C. Gerdes, “Autonomous vehicle control at the limits of handling,” Int. J. Veh. Auton. Syst., vol. 10, no. 4, pp. 271–296, 2012, doi: 10.1504/IJVAS.2012.051270.

[14] W. C. Mitchell, R. Schroer, and D. B. Grisez, “Driving the traction circle,” SAE Tech. Pap., no. 724, 2004, doi: 10.4271/2004-01-3545.

[15] N. R. Kapania, J. Subosits, and J. C. Gerdes, “A Sequential Two-Step Algorithm for Fast Generation of Vehicle Racing Trajectories,” J. Dyn. Syst. Meas. Control. Trans. ASME, vol. 138, no. 9, 2016, doi: 10.1115/1.4033311.

[16] AASHTO, A Policy on Geometric Design of Highways and Streets, 7th ed. Washington, D. C., 2018.

[17] P. A. Theodosis and J. C. Gerdes, “Generating a racing line for an autonomous racecar using professional driving techniques,” in ASME 2011 Dynamic Systems and Control Conference (DSCC 2011), 2011, pp. 853–860, doi: 10.1115/DSCC2011-6097.

[18] P. A. Theodosis and J. C. Gerdes, “Nonlinear optimization of a racing line for an autonomous racecar using professional driving techniques,” in ASME 2012 5th Annual Dynamic Systems and Control Conference Joint with the JSME 2012 11th Motion and Vibration Conference (DSCC 2012-MOVIC 2012), 2012, pp. 235–241, doi: 10.1115/DSCC2012-MOVIC2012-8620.

[19] J. Villagra, V. Milanés, J. Pérez, and J. Godoy, “Smooth path and speed planning for an automated public transport vehicle,” Rob. Auton. Syst., vol. 60, pp. 252–265, 2012, doi: 10.1016/j.robot.2011.11.001.

[20] H. A. Hamersma and P. S. Els, “Longitudinal vehicle dynamics control for improved vehicle safety,” J. Terramechanics, vol. 54, pp. 19–36, 2014, doi: 10.1016/j.jterra.2014.04.002.

[21] “Test Track.” https://www.larson.psu.edu/about/test-track.aspx (accessed Apr. 08, 2021).

[22] R. Solea and U. Nunes, “Trajectory planning with velocity planner for fully-automated passenger vehicles,” in 2006 IEEE Conference on Intelligent Transportation Systems (ITSC), 2006, pp. 474–480, doi: 10.1109/itsc.2006.1706786.